Radiation Spectra of ^{111}In, ^{113m}In and ^{114m}In

Jiri Stepanek, Samy A. Ilvonen, Antti A. Kuronen, Juha S. Lampinen, Sauli E. Savolainen and Petteri J. Välimäki

From the Institute of Medical Radiobiology, Paul Scherrer Institute, Villigen-PSI, Switzerland (J. Stepanek), the Electromagnetics Laboratory, Helsinki University of Technology, Helsinki (S.A. Ilvonen), Laboratory of Computational Engineering, Helsinki University of Technology, Espoo (A.A. Kuronen), the Departments of Radiology (J.S. Lampinen), Radiology and Laboratory Medicine (S.E. Savolainen), Clinical Neurophysiology, Medical Engineering Centre and Laboratory of Clinical Physiology, Helsinki University Central Hospital, Helsinki (P.J. Välimäki), Finland

Correspondence to: Jiri Stepanek, Institute of Medical Radiobiology (IMR), University of Zurich, Paul Scherrer Institute, CH-5232 Villigen-PSY, Switzerland Fax: + 41 56 31 04 412

Acta Oncologica Vol. 39, No. 6, pp. 667–671, 2000

The radiation spectra of ^{111}In, ^{113m}In, and ^{114m}In are calculated with the Monte Carlo computer program IMRDEC. The relaxation probabilities are taken from the EADL file of the Lawrence Livermore National Laboratory. Because this file does not include data for some *N* and *O* transitions, these were additionally determined by applying the Kassis rule. Two schemes are applied to calculate the transition energies: 1) a simple $(Z+1)/Z$ scheme, and 2) accurate calculation solving the relativistic Dirac equations. It is shown that using the extended set of relaxation probabilities leads to generation of many additional low-energy Auger and CK electrons if the $(Z+1)/Z$ rule is applied. On the other hand, the emissions of almost all these electrons are rejected if their energies are calculated solving the Dirac equations taking into consideration realistic electron vacancies.

Received 29 September 1999
Accepted 7 July 2000

In the past, the radiation spectra of ^{111}In and ^{113m}In were calculated by Howell (1). He extended his set of relaxation probabilities for ^{111}In by applying the Kassis rule (2) and applied the $(Z+1)/Z$ rule (3) to calculate the transition energies. This rule uses the electron binding energies precalculated for atoms in ground state, i.e. without any consideration of the realistic electron vacancy distribution during the Auger cascade. Therefore the application of this rule can lead to overestimation of energies of transitions between the outermost atomic subshells.

The recently developed computer program IMRDEC (4) allows the optional use of either the $(Z+1)/Z$ rule or the energy calculation solving the Dirac equations, calculating the transition energies as the difference between the total atomic energies before and after the transition. One of the aims of this work is therefore to investigate the effects of extending the relaxation probabilities as well as the energy effects by calculating the Auger and fluorescence spectra (a) with the original EADL file (5) which does not include relaxation probabilities between some *N* and *O* subshells, (b) applying the Kassis rule to extend the relaxation probabilities to all subshells, (c) applying the $(Z+1)/Z$ rule, and (d) calculating the transition energies quantum mechanically.

RADIATION SPECTRA

The decay spectra of ^{111}In, ^{113m}In and ^{114m}In were calculated with the computer program IMRDEC (4). The ^{111}In decays with a halftime of 2.8 days by electron capture (EC) followed by internal conversion (IC) to ^{111}Cd. The EC leads, on average, to 1.0 and IC to 0.16 vacancies in the electron shells per decay. The vacancies generated by the EC process are filled considering the isolated atom. Then the left vacancies together with vacancies generated by the IC process are filled taking into consideration the condensed phase. The ^{113m}In decays with a halftime of 1.66 h to ^{113}In by internal conversion. The generated electron vacancies (on average 0.36 per decay) were filled taking the condensed phase into consideration. The ^{114m}In decays with a halftime of 4.95 days with a branching ratio of 0.0325 to ^{114}Cd and with that of 0.9675 to ^{114}In. The decay to ^{114}Cd proceeds by electron capture (1.0 electron vacancy per decay) and internal conversion (0.0074 electron vacancy per decay). As in the case of ^{111}In, the fluorescence and electron cascades resulting from the EC process are calculated taking into consideration the isolated atom, whereas the left vacancies together with IC vacancies are filled in a second step taking into consideration the condensed phase.

 ISSN 0284-186X

All calculations were performed using the Monte Carlo option of IMRDEC code, taking into consideration 10^4 histories (decays). The decay schemes were taken from the ENSDF library of Brookhaven National Laboratory (6). The internal conversion coefficients required to generate the electron vacancies resulting from the IC process were taken from the INCOCO-00 file, recently generated by Stepanek (7). The relaxation probabilities were taken from the EADL file of the Lawrence Livermore National Laboratory (5). Because these probabilities were calculated considering a fully occupied atom assuming a single electron vacancy that has to be filled, the procedure of Krause & Carlson (8) was applied to correct them taking into consideration the realistic vacancy distribution. The EADL file does not include the relaxation probabilities for second and third outermost subshells. Therefore, these were estimated using a simple Kassis rule (2) based on the number and distribution of electrons available for the transition. This rule was checked calculating the missing N_6, N_7, O_2, and O_3 shells of ^{158}Gd quantum mechanically using the *jj*-coupling scheme by Chen from the Lawrence Livermore National Laboratory. In both cases, the total number of emitted Auger + CK electron was 9.7. Furthermore, the comparison of spectra has shown only minor differences (see Stepanek & Rivard (9)). The transition energies were calculated by a) applying the $(Z+1)/Z$ rule (3), and b) calculating them as the difference between the total energies of the atom before and after the cascade, allowing for

Table 1

Spectra of ^{113m}In and ^{114m}In: Condensed phase

Process	^{113m}In						^{114m}In	
	Present(1)		Howell		Present(2)		Present(2)	
	Av. Energy (eV)	Yield	Av. energy (eV)	Yield	Av. energy (eV)	Yield	Av. energy (eV)	Yield
Auger KLL	$2.01\times 10^{+4}$	2.91×10^{-2}	$1.98\times 10^{+4}$	2.59×10^{-2}	$2.01\times 10^{+4}$	3.00×10^{-2}	$2.00\times 10^{+4}$	4.52×10^{-2}
Auger KLX	$2.24\times 10^{+4}$	2.24×10^{-2}	$2.32\times 10^{+4}$	1.28×10^{-2}	$2.35\times 10^{+4}$	1.34×10^{-2}	$2.34\times 10^{+4}$	1.87×10^{-2}
Auger KKX	$2.67\times 10^{+4}$	1.38×10^{-3}	$2.68\times 10^{+4}$	1.20×10^{-3}	$2.69\times 10^{+4}$	1.60×10^{-3}	$2.68\times 10^{+4}$	1.76×10^{-3}
CK LLX	$2.64\times 10^{+2}$	4.71×10^{-2}	$1.97\times 10^{+2}$	4.48×10^{-2}	$2.47\times 10^{+2}$	4.57×10^{-2}	$2.05\times 10^{+2}$	8.44×10^{-2}
Auger LLM	$2.73\times 10^{+3}$	2.43×10^{-1}	$2.71\times 10^{+3}$	2.44×10^{-1}	$2.69\times 10^{+3}$	2.41×10^{-1}	$2.69\times 10^{+3}$	5.50×10^{-1}
Auger LMX	$3.21\times 10^{+3}$	5.88×10^{-2}	$3.20\times 10^{+3}$	5.99×10^{-2}	$3.20\times 10^{+3}$	6.38×10^{-2}	$3.19\times 10^{+3}$	1.34×10^{-1}
Auger LXY	$3.71\times 10^{+3}$	3.84×10^{-3}	$3.70\times 10^{+3}$	3.40×10^{-3}	$3.68\times 10^{+3}$	3.20×10^{-3}	$3.69\times 10^{+3}$	8.74×10^{-3}
CK MMX	$1.26\times 10^{+2}$	2.72×10^{-1}	$1.24\times 10^{+2}$	2.73×10^{-1}	$8.98\times 10^{+1}$	2.49×10^{-1}	$8.83\times 10^{+1}$	5.65×10^{-1}
Auger MXY	$3.74\times 10^{+2}$	6.22×10^{-1}	$3.76\times 10^{+2}$	6.22×10^{-1}	$3.26\times 10^{+2}$	6.20×10^{-1}	$3.30\times 10^{+2}$	$1.41\times 10^{+0}$
CK NNX	$3.43\times 10^{+1}$	7.88×10^{-1}	$3.58\times 10^{+1}$	7.38×10^{-1}	$5.80\times 10^{+1}$	6.95×10^{-1}	$5.74\times 10^{+1}$	$1.32\times 10^{+0}$
Auger NXY	$1.04\times 10^{+1}$	$2.35\times 10^{+0}$	$1.63\times 10^{+1}$	$2.30\times 10^{+0}$	$6.07\times 10^{+1}$	$1.65\times 10^{+0}$	$5.68\times 10^{+0}$	$3.61\times 10^{+0}$
CK OOX	$1.48\times 10^{+0}$	$2.67\times 10^{+0}$						
$K_{\alpha 1}$ x-rays	$2.42\times 10^{+4}$	1.33×10^{-1}	$2.42\times 10^{+4}$	1.33×10^{-1}	$2.43\times 10^{+4}$	1.32×10^{-1}	$2.42\times 10^{+4}$	1.98×10^{-1}
$K_{\alpha 2}$ x-rays	$2.40\times 10^{+4}$	7.04×10^{-2}	$2.40\times 10^{+4}$	6.98×10^{-2}	$2.41\times 10^{+4}$	7.18×10^{-2}	$2.40\times 10^{+4}$	1.07×10^{-1}
$K_{\beta 1}$ x-rays	$2.73\times 10^{+4}$	2.32×10^{-2}	$2.73\times 10^{+4}$	2.46×10^{-2}	$2.74\times 10^{+4}$	2.10×10^{-2}	$2.73\times 10^{+4}$	3.20×10^{-2}
$K_{\beta 2}$ x-rays	$2.78\times 10^{+4}$	7.38×10^{-3}	$2.79\times 10^{+4}$	6.10×10^{-3}	$2.79\times 10^{+4}$	8.00×10^{-3}	$2.79\times 10^{+4}$	1.25×10^{-2}
$K_{\beta 3}$ x-rays	$2.72\times 10^{+4}$	1.14×10^{-2}	$2.72\times 10^{+4}$	1.13×10^{-2}	$2.73\times 10^{+4}$	9.90×10^{-3}	$2.72\times 10^{+4}$	1.56×10^{-2}
$K_{\beta 4}$ x-rays	$2.79\times 10^{+4}$	4.00×10^{-5}					$2.68\times 10^{+4}$	3.25×10^{-6}
$K_{\beta 5}$ x-rays	$2.75\times 10^{+4}$	2.50×10^{-4}			$2.76\times 10^{+4}$	$2.00\times 10^{+4}$	$2.75\times 10^{+4}$	3.07×10^{-4}
L x-rays	$3.37\times 10^{+3}$	2.27×10^{-2}	$3.35\times 10^{+3}$	1.40×10^{-2}	$3.37\times 10^{+3}$	2.01×10^{-2}	$3.38\times 10^{+3}$	5.00×10^{-2}
M x-rays	$4.27\times 10^{+2}$	8.40×10^{-4}			4.14×10^{-2}	1.30×10^{-3}	$4.03\times 10^{+2}$	1.83×10^{-3}
N+ x-rays	$7.27\times 10^{+1}$	7.10×10^{-4}			$1.37\times 10^{+2}$	3.00×10^{-4}	$6.74\times 10^{+1}$	4.71×10^{-2}
Int. Bremsstrahlung							4.70×10^{-2}	2.09×10^{-6}
IC photons	$2.52\times 10^{+5}$	6.42×10^{-1}	$2.52\times 10^{+5}$	$6.40\times 10^{+1}$	$2.52\times 10^{+5}$	6.42×10^{-1}	$7.12\times 10^{+7}$	2.20×10^{-1}
Neutrino							$1.09\times 10^{+4}$	3.25×10^{-2}
IC electrons	$1.32\times 10^{+4}$	3.58×10^{-1}	$1.32\times 10^{+4}$	3.60×10^{-1}	$1.32\times 10^{+4}$	3.58×10^{-1}	$1.42\times 10^{+5}$	8.12×10^{-1}
RT x-rays	$6.13\times 10^{+3}$	2.70×10^{-1}	$6.09\times 10^{+3}$	$2.60\times 10^{+3}$	$6.10\times 10^{+3}$	2.66×10^{-1}	$9.20\times 10^{+3}$	4.64×10^{-1}
Auger and CK electrons	$2.11\times 10^{+3}$	$7.10\times 10^{+0}$	$2.05\times 10^{+3}$	$4.30\times 10^{+0}$	$2.20\times 10^{+3}$	$3.61\times 10^{+0}$	$4.15\times 10^{+3}$	$7.75\times 10^{+0}$
Free-bound x-rays	$3.49\times 10^{+1}$	$7.45\times 10^{+0}$			$3.45\times 10^{+1}$	$4.44\times 10^{+0}$	$7.27\times 10^{+1}$	$9.47\times 10^{+0}$
Recoil	7.27×10^{-2}	$1.00\times 10^{+0}$			7.27×10^{-2}	$1.00\times 10^{+0}$	2.92×10^{-2}	$1.00\times 10^{+0}$
Total	$3.92\times 10^{+5}$				$3.92\times 10^{+5}$		$2.37\times 10^{+5}$	

Table 2

Spectrum of ^{111}In: Condensed phase

Process	Present(1)		Howell		Present(2)		Pomplun	
	Av. energy (eV)	Yield	Av. energy (eV)	Yield	Av. energy (eV)	Yield	Av. energy (eV)	Yield
Auger KLL	1.91× 10^{+4}	9.91× 10^{-2}	1.91× 10^{+4}	1.03× 10^{-1}	1.93× 10^{+4}	9.84× 10^{-2}	1.91× 10^{+4}	1.09× 10^{-1}
Auger KLX	2.23× 10^{+4}	4.05× 10^{-2}	2.23× 10^{+4}	3.94× 10^{-2}	2.25× 10^{+4}	4.35× 10^{-2}	2.24× 10^{+4}	4.36× 10^{-2}
Auger KKX	2.55× 10^{+4}	4.21× 10^{-3}	2.55× 10^{+4}	3.60× 10^{-3}	2.57× 10^{+4}	4.10× 10^{-3}	2.55× 10^{+4}	3.99× 10^{-3}
CK LLX	1.58× 10^{+2}	1.55× 10^{-1}	1.83× 10^{+2}	1.51× 10^{-1}	2.47× 10^{+2}	1.52× 10^{-2}	2.34× 10^{+2}	1.49× 10^{-1}
Auger LMM	2.59× 10^{+3}	7.99× 10^{-1}	2.59× 10^{+3}	8.35× 10^{-1}	2.60× 10^{+3}	8.03× 10^{-1}	2.57× 10^{+3}	8.25× 10^{-1}
Auger LMX	3.04× 10^{+3}	1.88× 10^{-1}	3.06× 10^{+3}	1.90× 10^{-1}	3.06× 10^{+3}	1.81× 10^{-1}	3.05× 10^{+3}	1.92× 10^{-1}
Auger LXY	3.53× 10^{+3}	1.19× 10^{-2}	3.53× 10^{+3}	1.09× 10^{-2}	3.54× 10^{+3}	1.05× 10^{-2}	3.53× 10^{+3}	1.06× 10^{-2}
CK MMX	1.10× 10^{+2}	8.61× 10^{-1}	1.25× 10^{+2}	9.15× 10^{-1}	1.03× 10^{+1}	8.57× 10^{-1}	8.19× 10^{+1}	9.14× 10^{-1}
Auger MXY	3.46× 10^{+2}	2.05× 10^{+0}	3.50× 10^{+2}	2.09× 10^{+0}	3.28× 10^{+2}	2.05× 10^{+0}	2.93× 10^{+2}	2.11× 10^{+0}
CK NNX	3.12× 10^{+1}	2.57× 10^{+0}	3.88× 10^{+1}	2.54× 10^{+0}	2.68× 10^{+1}	1.49× 10^{+0}	2.12× 10^{+1}	1.20× 10^{+0}
Auger NXY	2.61× 10^{+0}	7.66× 10^{+0}	8.47× 10^{+0}	7.82× 10^{+0}	5.18× 10^{+1}	3.63× 10^{-1}	7.34× 10^{+1}	7.79× 10^{-2}
$K_{\alpha 1}$ x-rays	2.31× 10^{+4}	4.54× 10^{-1}	2.32× 10^{+4}	4.63× 10^{-1}	2.33× 10^{+4}	4.58× 10^{-1}	2.32× 10^{+4}	4.54× 10^{-1}
$K_{\alpha 2}$ x-rays	2.29× 10^{+4}	2.41× 10^{-1}	2.30× 10^{+4}	2.40× 10^{-1}	2.31× 10^{+4}	2.37× 10^{-1}	2.30× 10^{+4}	2.43× 10^{-1}
$K_{\beta 1}$ x-rays	2.61× 10^{+4}	7.91× 10^{-2}	2.61× 10^{+4}	7.88× 10^{-2}	2.62× 10^{+4}	8.12× 10^{-2}	2.61× 10^{+4}	7.85× 10^{-2}
$K_{\beta 2}$ x-rays	2.66× 10^{+4}	2.42× 10^{-2}	2.66× 10^{+4}	1.86× 10^{-2}	2.67× 10^{+4}	2.56× 10^{-2}	2.66× 10^{+4}	2.01× 10^{-2}
$K_{\beta 3}$ x-rays	2.60× 10^{+4}	3.99× 10^{-2}	2.63× 10^{+4}	3.83× 10^{-2}	2.62× 10^{+4}	3.93× 10^{-2}	2.61× 10^{+4}	4.08× 10^{-2}
$K_{\beta 4}$ x-rays	2.67× 10^{+4}	1.10× 10^{-4}						
$K_{\beta 5}$ x-rays	2.63× 10^{+4}	6.90× 10^{-4}	2.63× 10^{+4}	1.10× 10^{-3}	2.64× 10^{+4}	1.50× 10^{-3}	2.63× 10^{+4}	6.90× 10^{-4}
L x-rays	3.20× 10^{+3}	7.34× 10^{-2}	3.23× 10^{+3}	4.99× 10^{-2}	3.25× 10^{+3}	7.83× 10^{-2}	3.25× 10^{+3}	6.51× 10^{-2}
M x-rays	3.94× 10^{+2}	3.04× 10^{-3}	3.56× 10^{+2}	3.00× 10^{-3}	4.31× 10^{+2}	2.50× 10^{-3}		
N+ x-rays	4.10× 10^{+1}	5.37× 10^{-2}			5.21× 10^{+1}	7.75× 10^{-1}		
Int. Bremsstrahlung	3.63× 10^{+0}	1.63× 10^{-4}			0.63× 10^{+0}	1.63× 10^{-4}		
IC photons	3.85× 10^{+5}	1.63× 10^{-4}	3.84× 10^{+5}	1.84× 10^{+0}	3.86× 10^{+5}	1.85× 10^{+0}	3.86× 10^{+5}	1.85× 10^{+0}
Neutrino	4.25× 10^{+5}	1.00× 10^{+0}			4.25× 10^{+5}	1.00× 10^{+0}		
IC electrons	2.77× 10^{+4}	1.57× 10^{-1}	2.45× 10^{+4}	1.60× 10^{-1}	2.74× 10^{+4}	1.55× 10^{-1}	2.74× 10^{+4}	1.55× 10^{-1}
RT x-rays	2.00× 10^{+4}	9.69× 10^{-1}	2.00× 10^{+4}	8.90× 10^{-1}	2.03× 10^{+4}	1.70× 10^{+0}	2.00× 10^{+4}	9.02× 10^{-1}
Auger and CK electrons	6.51× 10^{+3}	1.44× 10^{+1}	6.75× 10^{+3}	1.47× 10^{+1}	6.51× 10^{+3}	6.05× 10^{+0}	6.55× 10^{+3}	5.63× 10^{+0}
Free-bound x-rays	1.20× 10^{+1}	1.46× 10^{+1}			2.50× 10^{+1}	2.20× 10^{+0}		
Recoil	4.32× 10^{-2}	1.00× 10^{+0}			4.32× 10^{-2}	1.00× 10^{+0}		
Total	8.65× 10^{+5}				8.65× 10^{+5}			

the realistic vacancy distribution. This calculation was performed solving the relativistic Dirac's equations during the Monte Carlo cascade calculation. In contrast the $(Z+1)/Z$ rule is based on the use of electron binding energies precalculated in EADL allowing for the fully occupied atom, i.e. without any electron vacancies. Consequently, this scheme also allows transitions that are energetically not possible if the realistic vacancy distribution is considered. This effect is particularly obvious in the case of transitions between outer subshells, i.e. in the case of a large number of vacancies such that the $(Z+1)/Z$ rule becomes inaccurate.

Tables 1 and 2 display the calculated condensed mean decay spectra of all three nuclides. In Table 2 the results of Howell (1) and Pomplun from Kernforschungsanlage Jülich (personal communication) are also included for comparison. There is a good agreement between the present spectra calculated using $(Z+1)/Z$ rule (method (1)) and Howell's spectra. This is because the basic procedures used to calculate these spectra were similar. The small differences are due to different sources of the relaxation probabilities and electron binding energies. Here IMRDEC uses the presently most up-to-date and most consistent data. What is remarkable is the agreement in the total number of generated Auger and Coster-Kronig electrons (^{111}In: 14.4 calculated by IMRDEC and 14.7 calculated by Howell). Larger difference between average *NNX* energies (present: 2.61 eV, Howell: 8.47 eV) may be caused by using different electron binding energies for outer subshells. These are in the range of a few electronvolts and therefore less accurate. Pomplun does not use the $(Z+1)/Z$ rule to calculate transition energies. Instead, he precalculates these

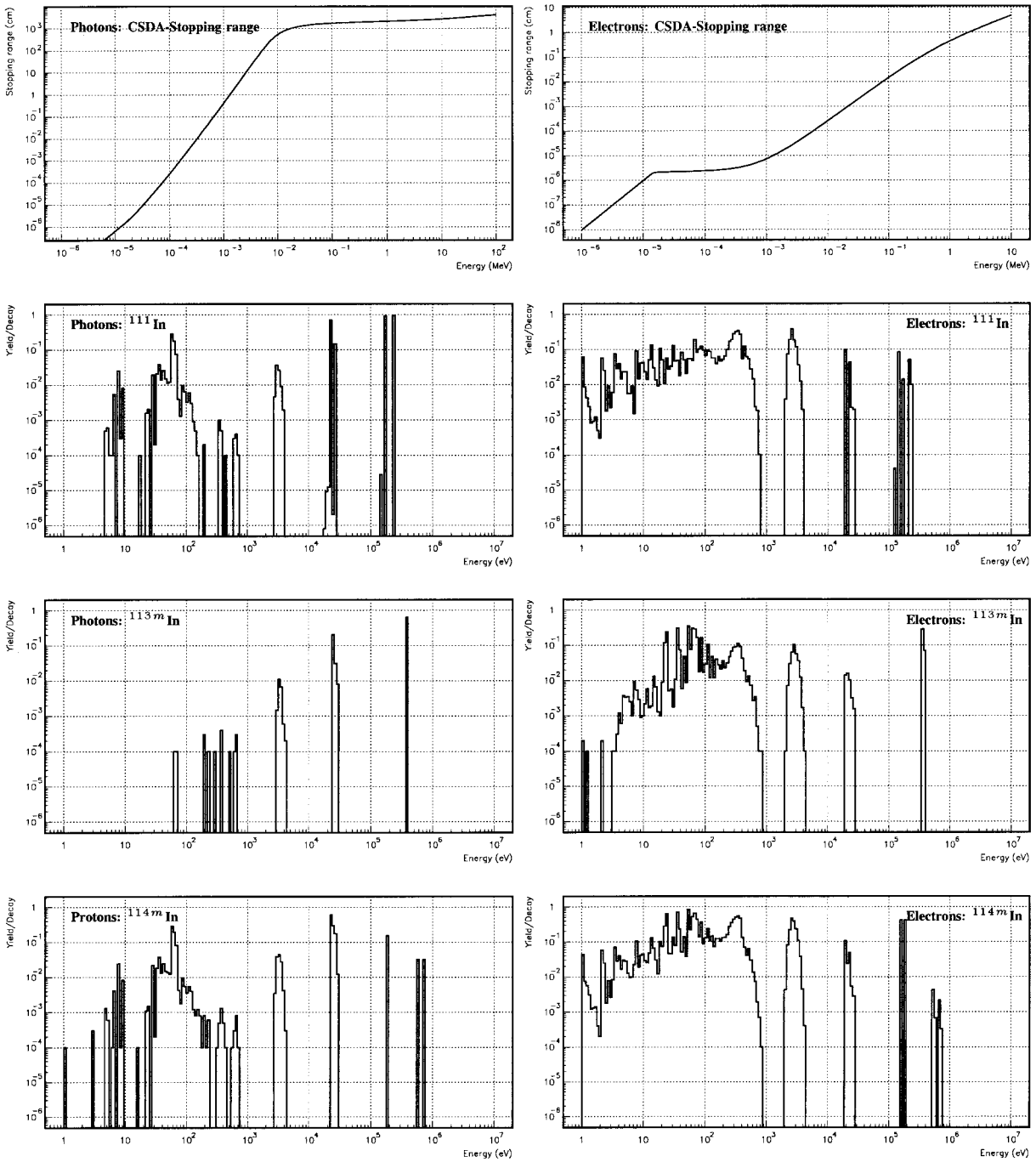

Fig. 1. CSDA stopping range of electrons in water and mean decay spectra of ^{111}In and ^{114m}In determined applying our method 2.

energies quantum mechanically for a large variety of vacancy distributions and then uses them in a subsequent Monte Carlo calculation. Therefore, his method is almost equivalent to our method (method 2). With the exception of *CK NNX* and Auger *NXY* yields, his spectra agree well with ours. Pomplun's yields are much lower, which indicates that probably some *N*- and *O*-shell transitions were not included in his calculation. In general, our and Pomplun's *NNX* and *NXY* yields are much lower than those calculated using method 1 and by Howell. This is the result of rejection of the transitions in which the quantum-mechanically calculated energy is zero or negative. A calculation of the spectra using method 1 but without extension of *N*-relaxation probabilities results in the same yields, with exception of *NNX*, which was 0.96 instead of 7.66 with the extended EADL file and 0.36 with the

extended EADL file but with method 2. The resultant total Auger and CK yields were 7.74, 14.4, and 6.05, respectively. This means that the use of the accurate method 2 leads to a rejection of more than all additional included *N*-shell transitions.

Table 1 displays the spectra of ^{113m}In and ^{114m}In. Again, also included is Howell's spectrum of ^{113m}In. As in the case of ^{111}In a good agreement is found comparing the present (method 1) and Howell's spectra. The only major difference is the inclusion of 2.66 *OOX*-Auger electrons in the present spectra. Subtracting this number from the total Auger and CK yield of 7.10 we get 4.43 electrons, which agrees well with Howell's total yield of 4.33. This indicates that Howell probably did not extend his set of relaxation probabilities to O_1 and O_2 shells. Also included are the spectra of ^{113m}In and ^{114m}In calculated using our method 2. With the exception of *NNX*, *NXY* and *OOX* yields, the agreement is good. The *NNX*, *NXY* and *OOX* yields are much smaller or zero because many of them, as in the case of ^{111}In, were rejected because of the negative energy of the transition. In the case of all three nuclides, we assume our method and Pomplun's method to be the most accurate.

The graphs in Fig. 1 display the stopping ranges of photons and electrons in water calculated with continuous stopping range approximation (CSDA). They were calculated using cross-sections from the EPDL and EEDL files of the Lawrence Livermore National Laboratory. These files include the photon and electron cross-sections down to 10 eV. Below this energy-cut, the stopping ranges were extrapolated applying the ICRU procedure. Also displayed are detailed mean Auger and Coster-Kronig spectra of ^{111}In, ^{113m}In and ^{114m}In calculated with our method 2. The spectra were bound into 200 energy bins in an energy range from 1 eV to 10 MeV.

CONCLUSIONS

All additional transitions calculated with the extended EADL file and applying the $(Z+1)/Z$ were rejected if accurate quantum-mechanical energy calculation was performed. This accurate method reduces even the number of Auger electrons calculated with the standard EADL file and $(Z+1)/Z$ rule. In both cases the electron spectra are reduced in the low-energy range.

REFERENCES

1. Howell RW. Radiation spectra for Auger-electron emitting radionuclides: Report No. 2 of AAPM Nuclear Medicine Task Group No. 6. Med Phys 1992; 19: 1371–83.
2. Kassis JAI, Adelstein SJ, Haydock C, Sastry KSR. Thallium-201: an experimental and theoretical radiobiological approach to dosimetry. J Nucl Med 1983; 34: 1164–75.
3. Chung MF, Jenkins LH. Auger electron energies of the outer shell electrons. Surf Sci 1970; 22: 479–85.
4. Stepanek J. A program to determine the radiation spectra due to a single atomic-subshell ionization by a particle or due to deexcitation or decay of radionuclides. Comp Phys Comm.
5. Cullen DE, Perkins ST. The 1991 Livermore Evaluated Atomic Data Library (EADL). Lawrence Livermore National Laboratory, Livermore CA. UCRL-50400 1991; 30.
6. Tuli K. Evaluated nuclear structure data file. Brookhaven National Laboratory Report BNL-NCS-51655-Rev 87; 1987.
7. Stepanek J. A new library containing internal-conversion coefficients.Comp Phys Comm 2000.
8. Krause MO, Carlson TA. Vacancy cascade in the reorganization of krypton ionized in an inner shell. Phys Rev 1967; 158: 28.
9. Stepanek J, Rivard M. Auger spectra and dosimetry of gadolinium-158. Med Phys 2000.